Physics Letters B 816 (2021) 136173

Contents lists available at ScienceDirect

Physics Letters B

www.elsevier.com/locate/physletb

Puzzle of collective enhancement in the nuclear level density

Deepak Pandit [a,d,*], Balaram Dey [b], Srijit Bhattacharya [c], T.K. Rana [a,d], Debasish Mondal [a], S. Mukhopadhyay [a,d], Surajit Pal [a], A. De [e], Pratap Roy [a,d], K. Banerjee [a,d], Samir Kundu [a,d], A.K. Sikdar [a], C. Bhattacharya [a,d], S.R. Banerjee [a]

[a] Variable Energy Cyclotron Centre, 1/AF-Bidhannagar, Kolkata 700064, India
[b] Department of Physics, Bankura University, Bankura, West Bengal 722155, India
[c] Department of Physics, Barasat Govt. College, Barasat, N 24 Pgs, Kolkata 700124, India
[d] Homi Bhabha National Institute, Training School Complex, Anushaktinagar, Mumbai 400094, India
[e] Department of Physics, Raniganj Girls' College, Raniganj 713358, India

ARTICLE INFO

Article history:
Received 5 March 2020
Received in revised form 28 October 2020
Accepted 18 February 2021
Available online 23 February 2021
Editor: D.F. Geesaman

Keywords:
Giant dipole resonance
Nuclear level density
Statistical theory of nucleus

ABSTRACT

The collective rotational enhancement in the nuclear level density (NLD) arising due to nuclear deformation is still not well understood due to sparse experimental findings. To address this issue, angular momentum (J) gated neutron, proton and GDR γ-ray spectra have been measured from two deformed nuclei (^{169}Tm and ^{185}Re) and one near spherical nucleus (^{201}Tl) by populating them around 26 MeV excitation energy. An enhanced yield compared to statistical decay is observed in all the three spectra (p, n, γ) for both the deformed nuclei but only statistical decay for near spherical nucleus. Intriguingly, the relative enhancement factors determined independently from all the spectra are very similar (≈ 10) for both the deformed nuclei. Moreover, the results indicate that the fadeout of the collective enhancement does not dependent strongly on the nuclear ground state deformation which is in stark contrast to the expectations of the phenomenological as well as microscopic calculations. The possible reasons for this discrepancy are discussed.

The nucleus is a complex quantum many body system where single particle as well as collective degrees of freedom constitutes elementary modes of excitation. Understanding the coexistence of these two contrasting facets of nuclear dynamics has been a fundamental problem in nuclear science [1,2]. The single particle excited states are described by the concept based on nucleons, comprising of neutrons and protons, occupying single particle orbits which are generated from their independent motion in a mean field potential [3]. The density of these quantum mechanical states increases rapidly with the increase in excitation energy and soon becomes extremely large [4–7]. The knowledge of the nuclear level density (NLD), defined as the number of excited levels per unit of excitation energy for a nucleus, is essential in numerous applications such as basic nuclear physics research, nuclear medicine [8], design of nuclear reactors, astrophysics [9] and fundamentally provides important information about nuclear thermodynamics [10]. On the other hand, the collective mode of excitation arises when the equilibrium shape of the nucleus deviates from spherical symmetry leading to ellipsoidal shapes [1]. The origin of this deformation is explained by the residual interaction between the nucleons occupying the single particle orbits in different configurations [11]. The key role of deformation is that it not only alters the spacing and order of the single particles states but also introduces rotational levels (collective degree of freedom) built on each intrinsic state resulting in an enhancement of the NLD [12,13]. The manifestation of the collective rotational enhancement in the NLD still remains a puzzling topic due to lack of experimental evidence. Up to now, a rather big uncertainty exists in the estimation of the magnitude of collective rotational enhancement and its fadeout with the increase in excitation energy [14–18].

The total collective enhancement in the NLD consists of vibrational and rotational excitations. The rotational enhancement, however, is much stronger and dominates for deformed nuclei [14–16]. The behavior of the rotational enhancement factor has been investigated quantitatively in different theoretical models. It has been predicted, assuming mirror and axial symmetry of the nucleus, that the level density should be $\sigma_\perp^2$ larger ($\sigma_\perp \approx 10$ for $A = 170$) [1,13,16] than the spherical nucleus, while the state densities (taking into account the degeneracy of each level) should only be $\sqrt{2/\pi}\ \sigma_\perp$ times greater [12,18], where $\sigma_\perp$ is the spin cutoff parameter perpendicular to the symmetry axis given as $\sigma_\perp^2 = I_\perp T/\hbar^2$.

* Corresponding author at: Variable Energy Cyclotron Centre, 1/AF-Bidhannagar, Kolkata 700064, India.
E-mail address: deepak.pandit@vecc.gov.in (D. Pandit).

https://doi.org/10.1016/j.physletb.2021.136173

$I_\perp$ is the rigid body moment of inertia perpendicular to the symmetry axis and $T = \sqrt{U/a}$ is the temperature. Besides, the fadeout of the enhancement has been predicted based on the nuclear shape transition. It is expected that a nucleus which is deformed at low energies would become spherical at higher energies. Consequently, any collective effect should disappear since the distinction between rotational and intrinsic motions becomes impossible. The calculations predict this shape transition at temperature $T \sim 1.7$ MeV corresponding to an excitation energy of 60 MeV for $A \sim 170$ nuclei having $\beta_2 = 0.3$ (ground state quadrupole deformation) [1,19]. However, the scarce experimental evidences have been contradictory [15,17] and no systematic data exists to verify the above predictions. Very recently, the experimental studies on neutron evaporation spectra from the rare earth nuclei have indicated the fadeout region around 15 MeV excitation energy ($T \sim 0.8$ MeV) [20–23], much below the predicted transition region.

Since the shapes of particle and γ spectra depend on the NLD, the collective enhancement should invariably manifest itself via both the decay channels. Hence to ascertain the fadeout region, angular momentum gated neutron, proton and the giant dipole resonance (GDR) spectra have been measured to probe the expected transition region. The GDR is macroscopically interpreted as the out of phase oscillation between the protons and the neutrons [24,25]. The damping of this motion results in the emission of high-energy γ rays (8–20 MeV). The measurements were performed for two deformed nuclei ^{169}Tm ($\beta_2 = 0.29$) and ^{185}Re ($\beta_2 = 0.22$) so as to understand the deformation effect on the fadeout region as well as on the enhancement factor. Finally, a near spherical ^{201}Tl ($\beta_2 = 0.04$) nucleus was also populated to establish the outcome arising only due to deformation. In this Letter, we present a clear signature of the enhancement in all the studied channels for both the deformed nuclei and only statistical decay for near spherical nucleus which help us to fathom out the interplay between collective mode and single-particle states.

The ^{169}Tm, ^{185}Re and ^{201}Tl compound nuclei were formed in the reactions ^{4}He + ^{165}Ho, ^{4}He + ^{181}Ta and ^{4}He + ^{197}Au, respectively, with 28 MeV alpha beams from the K-130 Cyclotron at the Variable Energy Cyclotron Centre, Kolkata. The initial excitation energies for ^{169}Tm, ^{185}Re and ^{201}Tl were 26.1, 25.2 and 25.9 MeV, respectively. High-energy γ rays from the decay of the GDR (≥ 5 MeV) were measured at an angle of 90° with respect to the beam axis employing the LAMBDA spectrometer arranged in a 7×7 array (49 BaF_2 detectors) [26]. The detector array was kept at a distance of 50 cm from the target. The neutrons were separated from the high-energy γ rays in the LAMBDA detectors using the time of flight (TOF) technique. The pile-up events were rejected by measuring the charge deposition over two integrating time intervals (30 ns and 2 μs). The proton spectra have been detected using a silicon detector (surface barrier) telescope kept at 140° angle with respect to the beam axis. The thickness of ΔE and E detectors were ∼ 50 and ∼ 5000 microns, respectively. The calibration of the telescope was done using ^{229}Th α-source. The neutron evaporation spectra were measured using a $5'' \times 5''$ liquid-scintillator [27] (BC501A) placed outside the scattering chamber at 150° angle with respect to the beam direction and at a distance of 150 cm from the target. The pulse shape discrimination (PSD) property of liquid scintillators was exploited for differentiating the neutrons and γ-rays. A 50-element low energy γ multiplicity filter [28] was used to estimate the angular momentum populated in the compound nucleus in an event-by-event mode as well as to get a fast start trigger for time-of-flight (TOF) measurements. The filter was split into two blocks of 25 detectors, each of which were placed on the top and bottom of a specially designed scattering chamber at a distance of 4.5 cm from the target in staggered castle-type geometry [22]. The high-energy γ rays (coming from the decay of the GDR), protons and neutrons were measured independently but in coincidence with the multiplicity filter when at least one detector each from the top and bottom blocks fired together. This 3-fold coincidence ensured the selection of events from the higher part of the compound nucleus (CN) spin distribution which considerably reduce the contribution of non-fusion events in the high-energy gamma ray spectra. The cyclotron RF time spectrum was also recorded with respect to the master trigger to ensure the selection of beam-related events.

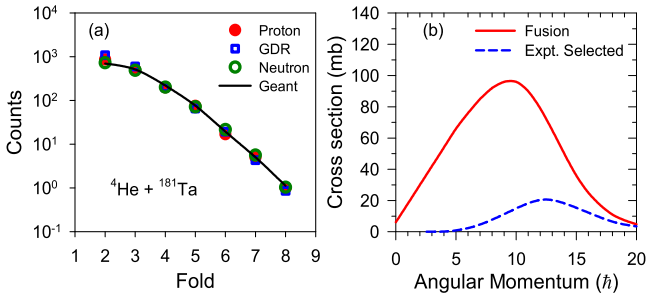

Fig. 1. (a) The experimental fold distributions (symbols) compared with GEANT simulation (continuous line). (b) The total fusion cross section and the experimentally selected cross section are compared with each other.

The energy of the emitted neutrons was determined using the TOF technique. The time resolution of the neutron detector was typically about 1.2 ns which gave an energy resolution of about 0.9 MeV at 10 MeV for the present setup. The efficiency of the neutron detectors were measured with the same experimental condition using a ^{252}Cf source. The scattered neutron contributions in the measured neutron spectra were also estimated and subtracted using the "shadow bar" technique by placing 60 cm thick high-density plastic (HDP) blocks in between the target and the detectors. The high-energy γ spectra were generated in offline analysis following the cluster summing technique [26,29]. The contribution from bremstrahlung was estimated and subtracted by fitting the exponential functions (e^{-E_γ/E_0}) in the γ energy interval 19–24 MeV. The slope parameter (E_0) was similar to the bremsstrahlung systematic [30], which has been verified in our previous experiments [22,31] at the same beam energy. The experimental fold (number of detectors fired in each event) distribution measured using the γ-multiplicity filter was converted to the angular momentum distribution through comparison with a detailed GEANT simulation [28]. The fold distributions measured by gating on the proton, GDR γ rays and neutron along with the selected angular momentum distribution for the reaction ^{4}He + ^{181}Ta populating ^{185}Re are shown in Fig. 1. The angular momentum ($< J >= 12 \pm 3\ \hbar$) gated neutron, proton and high-energy γ spectra from ^{169}Tm, ^{185}Re and ^{201}Tl in center of mass frame are shown in Fig. 2.

Most noteworthy is the enhanced yield in GDR (∼ 16 MeV), neutron (∼ 9 MeV) and proton spectra (∼ 11 MeV) (shown with arrow) for both the deformed nuclei but only statistical decay (no enhancement) is observed for near spherical nucleus. It should be emphasized here that at these excitation energies the enhanced region probed by different decay channels are predominantly from the first decay step enabling us to study the enhancement in a particular nucleus [22,32]. However, it is crucial to ascertain whether the enhanced yields are from compound nuclear decay. It has been shown earlier that, in alpha induced reactions, the high-energy GDR γ rays are emitted from a purely equilibrated statistical system by populating the same compound nucleus via different entrance channels [25]. Moreover, the non-fusion events are only associated with low angular momentum and γ rays less than 10 MeV because in these reactions the projectile/reaction products take away significant part of the input kinetic energy which leaves the residual nuclei with lower excitation energy and much

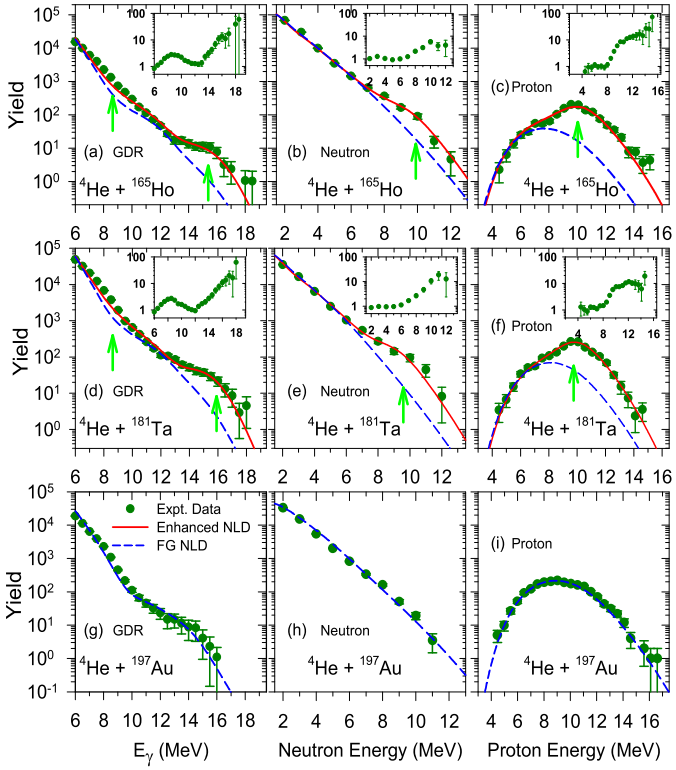

Fig. 2. The GDR and proton yield is per 0.5 MeV and the neutron yield is per MeV. The continuous and dashed lines represent the statistical model calculations with and without the collective enhancement in the NLD. The enhanced yields in GDR, neutron and proton spectra compared to statistical decay are displayed in inset and also shown with arrows.

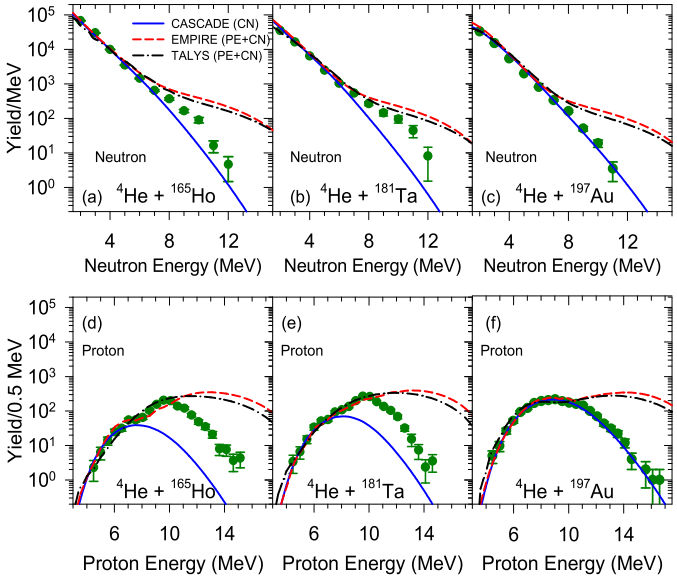

Fig. 3. Neutron (150°) and proton (140°) spectra have been compared with the corresponding pre-equilibrium + compound nucleus prediction of EMPIRE and TALYS code. The compound nucleus contribution from CASCADE code is also shown.

smaller angular momentum compared to the compound nucleus [33]. Since, in our experiment, we have selected the higher part of the spin distribution, the high-energy GDR γ ray around 16 MeV can only arise from fully energy equilibrated compound nucleus. In order to understand the contribution of pre-equilibrium emission in the particle spectra, we have performed EMPIRE 3.2.3 and TALYS 1.95 code calculations which provide pre-equilibrium contribution corresponding to inclusive spectrum (Fig. 3). As can be seen, the predicted pre-equilibrium contribution is very similar for all three nuclei selected in this experiment. However, the experimental data is completely different from those predicted by the pre-equilibrium emission. The enhancements observed in ^{181}Ta and ^{165}Ho reactions are also very dissimilar compared to pre-equilibrium emission. We tried to fit the observed enhanced spectra by changing the pcross parameter in EMPIRE code from 0.5 to 1.5 and M1 constant parameter from 0 to 100 in the TALYS code. But it was not possible to represent the spectra by pre-equilibrium emission as the nature of experimental and theoretical spectra are completely different due to selection of high spin distribution. The EMPIRE calculation with pcross 1.3 and TALYS with default parameter are shown in Fig. 3. The loss of angular momentum due to pre-equilibrium emission in alpha induced reactions has been studied earlier [34,35]. It has been shown that the pre-equilibrium high energy neutrons take away much higher angular momentum compared to statistical decay. At 28 MeV incident energy (as in our case), a pre-equilibrium neutron or proton emission in the energy range 8–14 MeV will take away large angular momentum (since 2/3 of the incident energy is lost after taking into account the binding energy of the nucleons) whereas a statistical decay takes away around 0.4–0.5 $\hbar$ [34] depending on the spin-dependent level-density. Thus, a pre-equilibrium decay will populate the residual nuclei at much lower angular momentum compared to the compound nucleus. The fold distributions (Fig. 1) obtained by gating on the proton, neutron and GDR spectra overlap with each other (for all the reactions) which suggest similar spin distribution of the residual nuclei populated via different channel emphasizing the compound nuclear decay.

In order to obtain a quantitative estimate of the enhancement factor, the data have been compared with the statistical Hauser-Feshbach model. The individual particle transmission coefficients were calculated by solving the Schrodinger equation with an optical potential for the particle-nucleus interaction. The potential parameters for neutron, proton, and alpha were taken from Refs. [36], [37] and [38], respectively. The intrinsic level density used in the modified version of the CASCADE code [39,40] is given as

$$\rho_{int}(E^*, J) = \frac{2J+1}{12\theta^{3/2}}\sqrt{a}\frac{\exp(2\sqrt{aU})}{U^2}. \quad (1)$$

Here, $U = E^* - \frac{J(J+1)\hbar^2}{2I_{eff}} - \Delta_p$ is the thermal energy. $\frac{J(J+1)\hbar^2}{2I_{eff}}$ is the energy bound in rotation and $\theta = \frac{2I_{eff}}{\hbar^2}$, where I_{eff} is the effective moment of inertia. The excitation energy is shifted back by the pairing energy Δ_p which is calculated using the relation $\Delta_p = \frac{12}{\sqrt{A}}$. The NLD parameter a is related to the single-particle density of states at the Fermi energy. The prescription of Ignatyuk [41] was used for the level density parameter which is given as $a = \tilde{a}[1 + (\Delta S/U)(1 - exp(-\gamma U))]$ where $\tilde{a} = A/k$, ΔS is the shell correction and γ is the shell damping factor. This parametrization takes into account the nuclear shell effects at low excitation energy and connects smoothly to the liquid drop regime at high excitation energy. It has been found to explain the high-energy γ ray spectra quite well in different mass regions both with heavy and light ion reactions [40,42].

The statistical model calculations for GDR, neutron and proton decay from all the studied nuclei are displayed in Fig. 2. It can be seen from Fig. 2 (g–i) that the statistical model calculation represents the GDR, neutron and proton spectra from ^{201}Tl excellently well using $k = 9.5 \pm 0.5$ MeV and ground state GDR values (one component Lorentzian function) [42]. The shell corrections for ^{201}Tl, ^{200}Tl and ^{200}Hg were taken as −8.36, −7.73 and −8.06 MeV, respectively, which were calculated within the CASCADE code by using the droplet model of Myers and Swiatecki [43] with the Wigner term. The good agreement of statistical

model prediction with experimental data for all the channels suggests that the evaporation process is indeed taking place from an equilibrated compound nucleus. The same calculation, on the other hand, failed to represent the data for the two deformed nuclei. Hence, in order to investigate the origin of this large yield in all the spectra, we have performed calculations by including the collective enhancement in the level density. Since, the residual nuclei in the decay chain of ^{169}Tm ($\beta_2 = 0.30$) and ^{185}Re ($\beta_2 = 0.22$) are also highly deformed (^{168}Tm ($\beta_2 = 0.29$), ^{168}Er ($\beta_2 = 0.29$), ^{184}Re ($\beta_2 = 0.23$) and ^{184}W ($\beta_2 = 0.24$)) [44], it is expected that rotational contribution in the NLD will be much larger than the vibrational contribution. This enables us to consider the total collective enhancement as rotational only. The energy dependent rotational enhancement factor was considered as a Fermi function given as

$$K_{rot} = (\sigma_{\perp}^2 - 1) f(U) + 1 \quad (2)$$

where $f(U) = (1 + e^{(U-E_{cr})/d_{cr}})^{-1}$. This form of the enhancement factor is different from the one used in our earlier work [22]. In the previous work, the neutron and GDR spectra were measured from ^{169}Tm which probed only the fadeout region and not below it (as can be seen in the inset of Fig. 2). In this work, the proton spectra have also been measured which probe the excitation energy below the transition region and display the Fermi function (inset of Fig. 2). This form makes it consistent with the theoretical predictions and similar to that employed in other experiments [15,23]. The magnitude of the enhancement was varied to explain the data by replacing $\sigma_{\perp}^2$ with α_1T, where α_1 was treated as a parameter. The enhancement factor parameters α_1, E_{cr} and d_{cr} were estimated from the particle spectra by considering a constant inverse level density parameter (k) which best explains the low energy part of the neutron spectra (below 8 MeV). In the case of γ spectra, the parameters were estimated considering the same inverse level density parameter and the ground state GDR parameters as extracted from the photo absorption cross section (two component Lorentzian function) [45,46] in accordance with Brink-Axel hypothesis and our recent GDR measurement on ^{169}Tm [47]. The values of k for ^{169}Tm and ^{185}Re were 8.5 ± 0.6 and 9.0 ± 0.5 MeV, respectively. The statistical model calculations for GDR, neutron and proton spectra, with and without the rotational enhancement factor are shown in Fig. 2. In order to emphasize the enhancement and its fadeout, the enhanced yields compared to statistical model calculations (without collective enhancement) are also displayed in inset of Fig. 2 (a–f). Since, both ^{169}Tm and ^{185}Re are deformed nuclei; the GDR is split into two components around 16 and 12 MeV corresponding to the vibration along short and long axis, respectively [45,46]. At 26 MeV excitation energy, the high-energy GDR component (16 MeV) will be dominant from the first stage of the compound nuclear decay which enables us to extract the enhancement in ^{169}Tm and ^{185}Re nuclei. The low energy component can arise from both compound nucleus as well as after neutron decay. The signature of the GDR decay after one neutron is indeed seen in the spectra. Interestingly, the enhancement factors used for ^{168}Tm and ^{184}Re to describe the neutron spectrum, simultaneously explain the γ spectrum between $E_\gamma = 7$ and 11 MeV (Fig. 2 (a, d)). This enhancement results from the emission of the GDR, after one neutron decay, when the low-energy GDR component explores the enhanced level density region. This simultaneous enhancement in γ and neutron spectra enables us to extract the enhancement in ^{168}Tm and ^{184}Re while the enhancement factors in ^{168}Er and ^{184}W are extracted from proton spectra.

Fig. 4a displays the experimentally determined enhancement factors from different spectra (logarithmic scale). The extracted parameters for different nuclei are almost similar and centered around $\alpha_1 = 15 \pm 3$, $E_{cr} = 10 \pm 2$ and $d_{cr} = 0.6 \pm 0.1$. As can be seen, the magnitude of the enhancements extracted independently

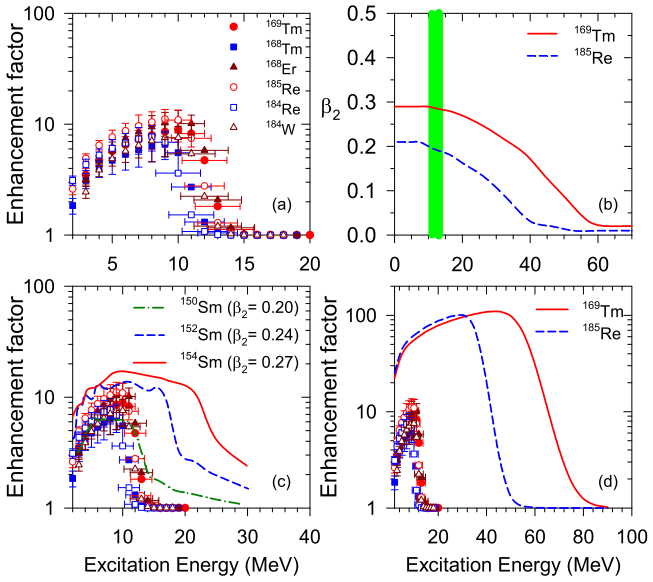

Fig. 4. (a) The enhancement factors extracted from GDR and particle spectra for different nuclei. (b) The variation of nuclear deformation with excitation energy displaying the shape transition ($\beta_2 \approx 0$). The green shaded region is the fadeout of the enhancement measured in the experiment. The experimental data have been compared with the predictions of (c) microscopic model [14] and (d) phenomenological calculation [15] of collective rotational enhancement.

from GDR, neutron and proton from both the deformed nuclei are ≈ 10. The results are consistent with the recent measurement of enhancement from the neutron evaporation spectra for ^{188}Os [23]. The data have also been compared with the estimates of microscopic calculation for Sm isotopes (similar deformation [44] as selected in our experiment) based on state densities (Fig. 4c) [14] and phenomenological calculation based on level densities (Fig. 4d) [15]. It is very interesting to find that the magnitude of the enhancements is very similar to the value predicted by the microscopic calculation but significantly smaller than the phenomenological estimates. It is observed that the values measured from emission spectra (p, n, γ) are comparable to the estimation based on state densities [18,14], whereas the enhancement values obtained from fragment production (≈ 70 at 10 MeV excitation energy) [15] and neutron resonances (≈ 50 for Dy isotopes [18,48]) are similar to the prediction based on level densities. It is also intriguing to find that the fadeout of the enhancement determined independently from the GDR, neutron and proton decay are also similar (Fig. 4a). These values of the critical energies for fadeout are, however, much smaller than the values predicted based on the nuclear shape transition when the nucleus becomes spherical and no longer supports rotational bands. The critical values for ^{169}Tm and ^{185}Re are about 60 and 40 MeV respectively (4b), calculated based on macroscopic–microscopic model [47,21], whereas the experimentally measured values are much smaller as shown with shaded region (10–14 MeV). It is important to note that although the shape transition energies are model dependent but they predict the fadeout strongly dependent on the nuclear ground state deformation as can be seen in Fig. 4(b–d). The experimental data, however, do not display such behavior as similar fadeout value is obtained for both ^{169}Tm and ^{185}Re inspite of having quite different deformation. As a matter of fact, a similar fadeout value of 12 MeV has also been obtained recently for ^{187}Os ($\beta_2 = 0.21$) from neutron evaporation spectra [23]. It needs to be mentioned that the collective enhancement factor in the microscopic approach is defined relative to the mean-field state density which describes the density of intrinsic states. The ratio of the total density to the mean-field density describes the additional contribution of rotational bands that are built on top of these intrinsic states. On the

other hand, experimentally one can only measure the relative enhancement factor based on the back-shifted Fermi gas model. The evaporation spectra are decided by the ratio of the level density of the daughter nucleus to the compound nucleus and may not offer a clear separation between single-particle and collective excitations. Thus, the extraction of the collective enhancement factor in the experiment and theory is totally different which may be the reason for the early fadeout of the enhancement seen in the experiment results. Apart from this, the discrepancy could be due to the finite size of the nucleus. The finite size effect introduces large thermal fluctuation in shape ($T \sim 0.8$ MeV [47]) which convolutes the static ground state deformation and may lead to the loss of collective rotational enhancement [47,21] much earlier. More observations are required especially in this transition region to understand the perplexing behavior of the enhancement factor and its fadeout. Characterizing the behavior of NLD in this excitation energy is extremely important in order to predict theoretically the cross sections for nuclei far off stability which are not accessible experimentally and essential in the field of nuclear astrophysics.

In summary, we present a systematic experimental evidence of the collective rotational enhancement in the NLD by measuring the GDR γ ray, neutron and proton spectra from highly deformed ^{169}Tm and ^{185}Re nuclei. The relative enhancement factors determined independently from the GDR, neutron and proton spectra for both the nuclei are around 10. The experimental observations also demonstrate that the fadeout of the enhancement is around 14 MeV excitation energy for both the deformed nuclei although having very different ground state deformation. This intriguing result indicates that the collective enhancement fadeout in the NLD does not depend strongly on the nuclear ground state deformation contrary to the current theoretical understanding.

Declaration of competing interest

The authors declare that they have no known competing financial interests or personal relationships that could have appeared to influence the work reported in this paper.

Acknowledgements

The authors gratefully acknowledge helpful discussions with Prof. S. M. Grimes and Prof. Subinit Roy for providing the surface barrier detector. S. R. Banerjee acknowledges financial assistance from Science and Engineering Research Board (Government of India) Grant No. CRG-2018-000336.

References

[1] A. Bohr, B.R. Mottelson, Nuclear Structure, vol. 1, Benjamin, New York, 1969, p. 2.
[2] T. Schafer, Nucl. Phys. A 928 (2014) 180.
[3] O. Haxel, J.H.D. Jensen, H.E. Suess, Phys. Rev. 75 (1949) 1766.
[4] H.A. Bethe, Phys. Rev. 50 (1936) 332.
[5] J.R. Huizenga, L.G. Moretto, Annu. Rev. Nucl. Sci. 22 (1972) 427.
[6] A.V. Ignatyuk, K.K. Istekov, G.N. Smirenkin, Sov. J. Nucl. Phys. 29 (1979) 450.
[7] N. Quang Hung, N. Dinh Dang, L.T. Quynh Huong, Phys. Rev. Lett. 118 (2017) 022502.
[8] H.R. Mirzaei, et al., J. Cancer Res. Ther. 12 (2016) 520.
[9] F.K. Thielemann, et al., Prog. Part. Nucl. Phys. 66 (2011) 346.
[10] E. Melby, et al., Phys. Rev. Lett. 83 (1999) 3150.
[11] J.P. Elliott, Proc. R. Soc. A 245 (1958) 128.
[12] S.M. Grimes, Phys. Rev. C 78 (2008) 057601.
[13] S.M. Grimes, Phys. Rev. C 88 (2013) 024613.
[14] C. Ozen, Y. Alhassid, H. Nakada, Phys. Rev. Lett. 110 (2013) 042502.
[15] A.R. Junghans, et al., Nucl. Phys. A 629 (1998) 635.
[16] G. Hansen, A.S. Jensen, Nucl. Phys. A 406 (1983) 236.
[17] S. Komarov, et al., Phys. Rev. C 75 (2007) 064611.
[18] S.M. Grimes, T.N. Massey, A.V. Voinov, Phys. Rev. C 99 (2019) 064331.
[19] A.L. Goodman, Phys. Rev. C 35 (1987) 2338.
[20] Pratap Roy, et al., Phys. Rev. C 88 (2013) 031601(R).
[21] K. Banerjee, et al., Phys. Lett. B 772 (2017) 105.
[22] Deepak Pandit, et al., Phys. Rev. C 97 (2018) 041301(R).
[23] G. Mohanto, et al., Phys. Rev. C 100 (2019) 011602(R).
[24] J.J. Gaardhoje, Annu. Rev. Nucl. Part. Sci. 42 (1992) 483.
[25] K.A. Snover, Annu. Rev. Nucl. Part. Sci. 36 (1986) 545.
[26] S. Mukhopadhyay, et al., Nucl. Instrum. Methods A 582 (2002) 603.
[27] K. Banerjee, et al., Nucl. Instrum. Methods A 608 (2009) 440.
[28] Deepak Pandit, et al., Nucl. Instrum. Methods A 624 (2010) 148.
[29] Deepak Pandit, et al., Phys. Lett. B 690 (2010) 473.
[30] H. Nifennecker, J.A. Pinston, Annu. Rev. Nucl. Part. Sci. 40 (1990) 113.
[31] Balaram Dey, et al., Phys. Lett. B 731 (2014) 92.
[32] Balaram Dey, et al., Phys. Lett. B 789 (2019) 634.
[33] D.R. Chakrabarty, et al., Phys. Rev. C 85 (2012) 044619.
[34] D.G. Sarantites, et al., Phys. Rev. C 17 (17) (1978) 601.
[35] M.J.A. de Voigt, et al., Nucl. Phys. A 379 (1982) 160.
[36] C.M. Perey, F.G. Perey, At. Data Nucl. Data Tables 17 (1976) 1.
[37] F.G. Perey, Phys. Rev. 131 (1963) 745.
[38] L. Mcfadden, G.R. Satchler, Nucl. Phys. A 84 (1966) 177.
[39] Srijit Bhattacharya, et al., Phys. Rev. C 78 (2008) 064601.
[40] Srijit Bhattacharya, et al., Phys. Rev. C 90 (2014) 054319.
[41] A.V. Ignatyuk, G.N. Smirenkin, A.S. Tishin, Sov. J. Nucl. Phys. 21 (1975) 255; Yad. Fiz. 21 (1975) 485.
[42] Deepak Pandit, et al., Phys. Lett. B 713 (2012) 434.
[43] W.D. Myers, W.J. Swiatecki, Ann. Phys. (N.Y.) 84 (1974) 186.
[44] P. Moller, et al., At. Data Nucl. Data Tables 59 (1995) 185.
[45] A.V. Varlamov, V.V. Varlamov, D.S. Rudenko, M.E. Stepanov, Atlas of Giant Dipole Resonances, INDC(NDS)-394, 1999 (unpublished); JANIS database.
[46] B.L. Berman, S.C. Fultz, Rev. Mod. Phys. 47 (1975) 713.
[47] Deepak Pandit, et al., Phys. Rev. C 99 (2019) 024315.
[48] Thomas Dossing, Sven Aberg, Eur. Phys. J. A 55 (2019) 249.